Available online at www.sciencedirect.com
ScienceDirect
Medical Laser Application 22 (2007) 199–206
Medical Laser Application
www.elsevier.de/mla

Near-infrared laser photothermal therapy of cancer by using gold nanoparticles: Computer simulations and experiment

Irina L. Maksimova[a,*], Garif G. Akchurin[a], Boris N. Khlebtsov[b], Georgy S. Terentyuk[c], Georgy G. Akchurin[a], Igor A. Ermolaev[a], Alexander A. Skaptsov[a], Ekaterina P. Soboleva[c], Nikolai G. Khlebtsov[a,b], Valery V. Tuchin[a]

[a]*Saratov State University, 83 Astrakhanskaya Street, Saratov, 410012, Russia*
[b]*Institute of Biochemistry and Physiology of Plants and Microorganisms, Russian Academy of Sciences, 13 Prospekt Entuziastov, Saratov, 410049, Russia*
[c]*First Veterinary Clinic, 98 Astrakhanskaya Street, Saratov, 410012, Russia*

Received 3 September 2007; accepted 5 September 2007

Abstract

We describe applications of silica(core)/gold(shell) nanoparticles to photothermal therapy of spontaneous tumor of cats and dogs. The laser irradiation parameters was optimized by preliminary experiments with laboratory rats. The temperature distribution in tissue and solution samples was measured with a thermal imaging system. It is shown that the temperature in the volume region of nanoparticles localization can substantially exceed the surface temperature recorded by the thermal imaging system. We demonstrate effective optical destruction of cancer cells by local injection of plasmon-resonant gold nanoshells followed by continuous wave (CW) semiconductor laser irradiation at wavelength 808 nm.

Keywords: Gold nanoparticles; Silica/gold nanoshells; Plasmon resonance; Cancer; Laser photothermal therapy

Introduction

It is commonly recognized to date that the unique optical properties of plasmon-resonant particles, together with the high specificity of biomolecular recognition, open new possibilities for applications in biomedical diagnostics [1], targeted drug delivery [2], optical imaging and photothermal therapy [3,4]. Recently, there appear the first reports [5,6] on optimization and optical amplification of laser heating based on light absorption by plasmon-resonant nanostructures.

Applications of plasmon-resonant nanostructures to biomedical science and practice are based on two principles: (1) the biospecific targeting of tissues or cells and (2) the optical plasmon resonance [1–5]. Addressed accumulation of particles within or near biological target can be achieved by passive or active targeting. In the first case, the nonfunctionalized inert particles are accumulated within a desired biological target according to the size-dependent penetration. For example, 130-nm silica/gold nanoshells can pass through the vessel walls leading to their accumulation in the surrounding tumor tissue [7]. The second (“active”) approach is based on the use of particles with the surface attached to biospecific probing molecules that can bind the target

*Corresponding author.
E-mail address: irina_mksmv@yahoo.com (I.L. Maksimova).

1615-1615/$ - see front matter © 2007 Elsevier GmbH. All rights reserved.
doi:10.1016/j.mla.2007.09.004

molecular sites. The surface molecular attachment procedure is called "functionalization" [8] and the term "conjugate" is often used to designate functionalized particles [9,10].

The optical plasmon resonance is caused by coherent oscillations of free metal electrons under electric component of illuminating light. These oscillations lead to the enhanced scattering and absorption of light at resonance wavelengths that are determined by poles of the dipole polarizability tensor. Depending on the particle design, the resonance wavelength can be tuned to the desired spectral band. For example, such a tuning can be achieved through variation of the core/shell ratio of silica/gold nanoshells [11,12]. The optical resonance can be used in two options: strongly localized heating or localized release of an encapsulated drug or some chemical substance. The first option presents a conceptual basis of photothermal therapy [4], whereas the second option is closely related to the addressed drug delivery technologies [2,13].

It is known that "the optical transparency window" of biotissues corresponds to the near infrared (NIR) region and is limited by 750–1100 nm with absorption coefficient less than 0.5 cm^{-1}. The lower bound corresponds to the absorption of red light by melanin and blood, whereas the upper window bound is determined by the water absorption spectrum. Spectral tuning of plasmon resonances to the NIR region of tissue transparency is a crucial point, and one needs photothermal technologies based on tunable plasmon-resonant nanostructures (within 750–1100 nm) instead of the usual colloidal gold nanospheres, possessing a weakly tunable resonance in the visible range (around 520–560 nm).

To make the photothermal therapy of cancer cells highly effective, one needs to ensure the correspondence between three important factors: the laser wavelength, the maximal absorbance of the gold nanostructures being used as selective labels, and the spectral transmittance of the biotissues treated by laser pulses. The size-dependent spectral tuning of gold nanospheres is not effective, so their use as photothermal labels is justified only at laser wavelengths near 520 nm. However, during transition to the NIR region (transparent for most biotissues), the use of single gold spheres does not seem effective because of the small normalized absorption. The use of gold nanorods and nanoshells as photothermal labels allows one to work in a broad spectral region, from 600 to 1500 nm, by varying the axial ratio of nanorods or the core(SiO_2)/shell(Au) ratio of nanoshells. For experiments described in this report, the plasmon-resonant nanoparticles (gold nanospheres, nanoshells and nanorods) were fabricated in the Laboratory of Nanoscale Biosensors, IBPPM RAS.

Theoretical modeling

Spatial distribution of the absorbed laser radiation

The theoretical part of our study was to simulate the spatial distribution of light absorbance related to the process of electromagnetic wave propagation through a system of discrete scattering particles with consideration of multiple scattering effects. By using the computer Monte Carlo codes, we calculated diffuse scattering in the systems of gold nanoshells for laser radiation (wave length 808 nm).

It is known that the absorption and scattering spectra of plasmon-resonant particles strongly depend on their particle size and shape. By changing the diameter of spherical gold particles, it is possible to obtain spectral characteristics with the center of absorption peak in different parts of visible spectrum. Additional possibilities for obtaining the desired spectral characteristics come from using the suspension of nonspherical or layered particles. In these cases, the plasmon resonance shifts to the NIR region, where the biological tissue transparency window is located.

Fig. 1 shows the spatial distribution of absorption intensity for silica/gold nanoshells in water. The spectral dependence of the gold optical constants was taken from a spline corresponding to the experimental data [14–16]. The extinction and scattering efficiencies are defined as the ratio of the integral optical cross sections to the geometrical cross section. For the silica core diameters and the shell thicknesses about 140 and 15 nm, respectively, the extinction peak is localized near 810 nm. The variations in particle concentration and accordingly in the multiplicity of scattering lead to the change in the spatial distribution of absorption. The laser radiation is mainly absorbed near the sample surface and it is strongly scattered in the case of high particle concentration (Fig. 1a). With the small concentrations of particles, the radiation penetrates more deeply (Fig. 1b).

Calculation of the temperature fields

To calculate the spatial distribution of the temperature, we employed the two-dimensional Poisson equation as a mathematical model. The axial symmetry of our problem allows to restrict the solution by two-dimension of the Poisson equation written in cylindrical coordinates:

$$\mathrm{div}(\lambda\,\mathrm{grad}(T(r,z)) = Q(r,z), \tag{1}$$

where λ is the coefficient of thermal conductivity, $T(r, z)$ is the temperature, $Q(r, z)$ is the power of the internal heat sources. The thermal boundary conditions have the following forms:

$$\lambda\frac{\partial T}{\partial r}|_{r=R} = \alpha_1(T|_{r=R} - T_0), \quad \lambda\frac{\partial T}{\partial z}|_{z=0} = \alpha_2(T|_{z=0} - T_0). \tag{2}$$

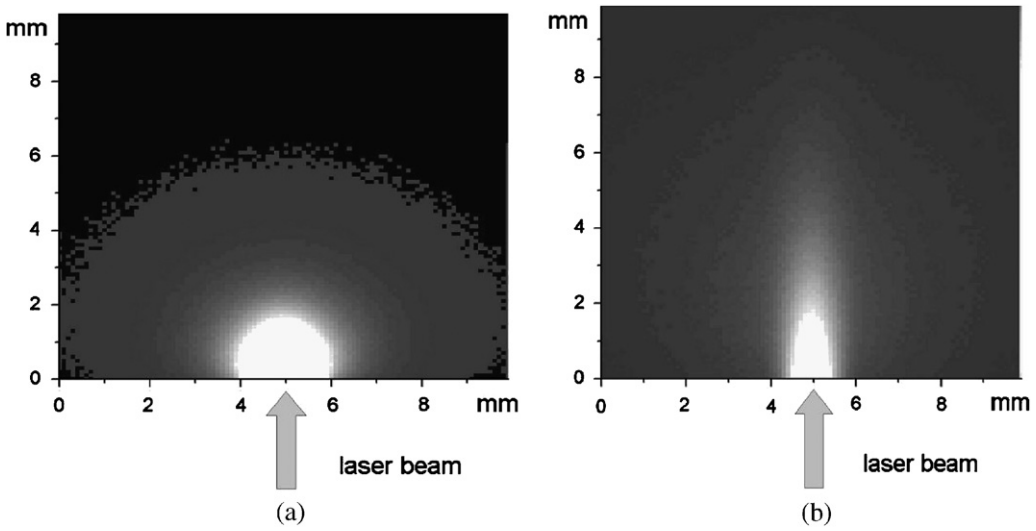

Fig. 1. Computer simulation of the spatial distribution of absorption intensity: (a) particle concentration of $5 \times 10^9\,\mathrm{ml}^{-1}$ and (b) particle concentration of $1 \times 10^9\,\mathrm{ml}^{-1}$. The incident light propagates from bottom to top (positive z-direction), the scattered layer is supposed to be infinite for x- and y-directions.

Here, α_1 and α_2 are the coefficients of heat transfer at the side boundaries of the computational domain and T_0 is the external temperature of surrounding medium ($T_0 = 25\,^{\circ}\mathrm{C}$).

The Poisson equation (1) was solved by the Galerkin finite-element method. The temperature was approximated by a linear combination of the basis (shape) functions on the linear triangular finite elements. To solve the system of algebraic equations, we used the Gauss method as applied to band matrices. The calculations were carried out with a nonuniform finite-element grid possessing 1800 points. Fig. 2a, b shows isotherms of the stationary temperature fields.

Experimental studies

Experimental studies included the determination of spatial distribution of temperature with different depth and concentrations of nanoparticles in samples of biological tissues.

Infrared imager IRISYS 4010 (InfraRed Integrated System Ltd., UK) was used for noncontact measurements and recording the temperature of samples under study. A computer complex Imager IRISYS 4000 (InfraRed Integrated System Ltd., UK) was used for thermogram analysis.

Fig. 3 shows the measured thermograms for colloidal solution of silica/gold nanoshells in cylindrical test-tube. The laser radiation propagates to the end of test-tube parallel with its axes. The thermogram was recorded in lateral direction of test-tube. Such a configuration allows to obtain a depth profile of temperature.

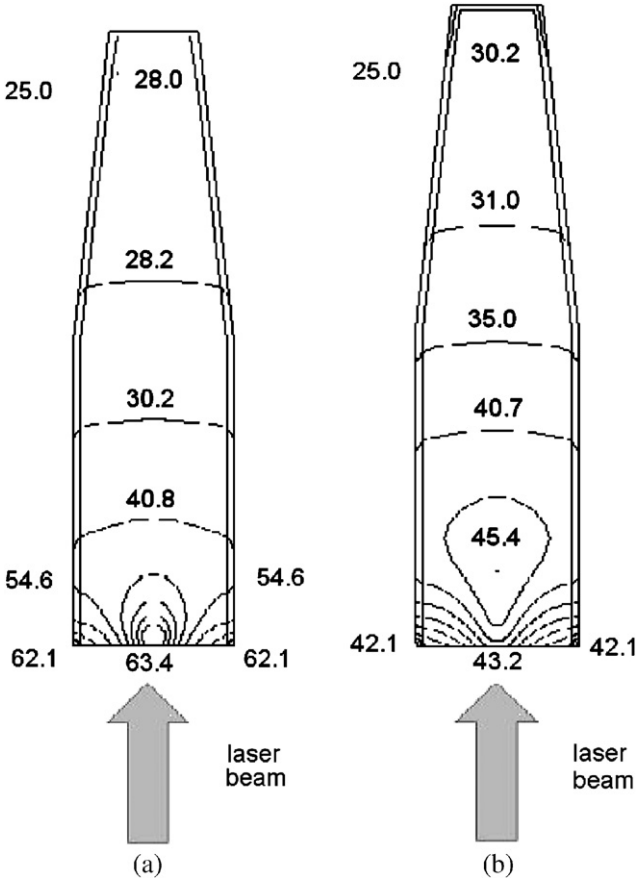

Fig. 2. The stationary isotherms calculated by two-dimensional Poisson equation for two-dimensional axial symmetrical model of an Eppendorf vial. The spatial distribution of the thermal sources $Q(r, z)$ was obtained from computer simulations shown in Fig. 1.

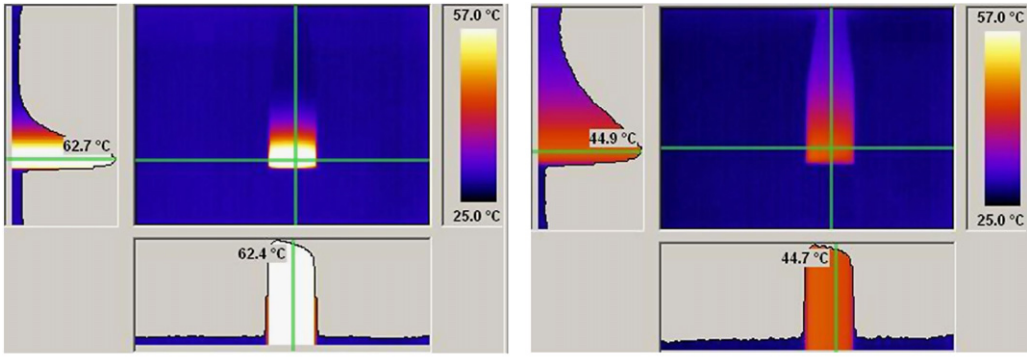

Fig. 3. Thermogram of plasmon-resonant nanoshells in a standard Eppendorf vial (1.5 ml) after 2 min irradiation with a laser beam power of 2 W: (a) particle concentration is 5×10^9 ml^{-1} and (b) particle concentration was decreased to 0.61×10^9 ml^{-1}. The incident light propagates from bottom to top.

All samples were irradiated by semiconductor laser PhotoThera Laser System operating at 808 nm and output power 2 W for continuous wave (CW) mode. The Gaussian beam diameter at a level $1/e^2$ was about 5 mm and the power density was about 10 W/cm^2.

In vivo thermal laser effect on biotissues with nanoparticles

We have measured also the temperature characteristics of animal skin at hypodermic and intramuscular introduction of gold nanoparticle *in vivo* (Figs. 4 and 5).

For experiments with the white laboratory rats we used a general anesthesia by 0.2 ml zoletil (Salute Animale Virbas). The experimental animals were fixed at the horizontal position supine with hair shaved off. Every animal was labeled by a symmetrical centerline of stomach as shown in Fig. 4. Three sections to the left from the centerline were used to control the heating under laser radiation without nanoparticles. The control sections in figures are marked by asterisks ("●", "●●", and "●●●"). About 0.1 ml of the nanoshell suspension was injected in three sections to the right from the centerline. In the section marked as "X", "XX", and "XXX", the injections were intradermal, subcutaneous, and intramuscular, respectively. The injection depth was about 5 mm, the laser power was 2.5 W, and the distance between fiber and skin surface was about 15 mm. Histological examination of tissues from all sections was carried out after laser irradiation and temperature registration. The coagulation of tissue marked by X symbol had been observed visually already after 10 s of irradiation.

The control section (without nanoparticles) of rat tissues was heated up to 46 °C. This temperature cannot lead to irreversible injuries of tissues, although such heating can lead to damage of cells in case of sufficiently prolonged treatment.

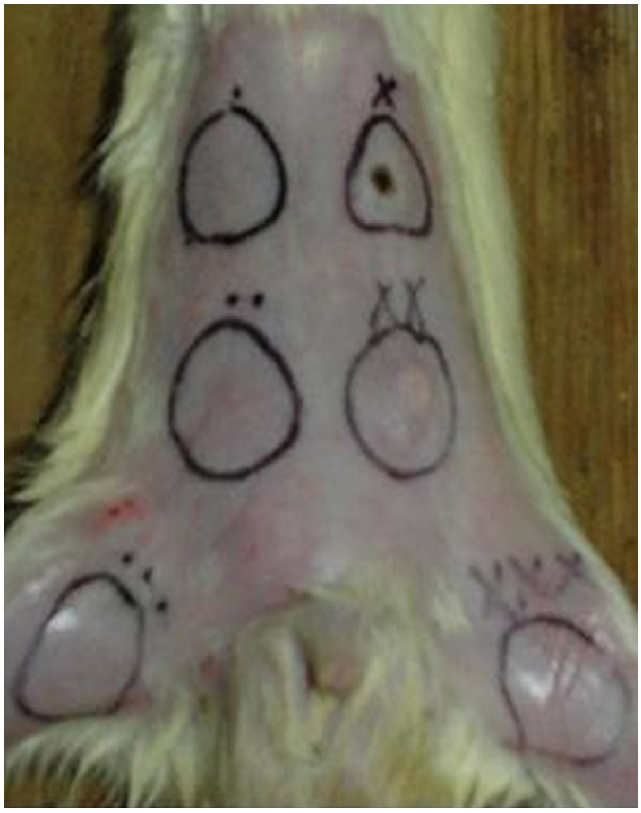

Fig. 4. Laser photothermolysis (800 nm) of superficial rat tissue with intradermal injection of gold nanoparticles. Symbols ●, ●●, and ●●● stand for control (without nanoparticles); symbols X, XX designate the hypodermic injection of 0.1 ml nanoparticle solution; symbols XXX designate the intramuscular injection of 0.1 ml nanoparticles to depth of about 5 mm.

In the case of the intramuscular introduction (section "XXX") we did not observe significant changes in the

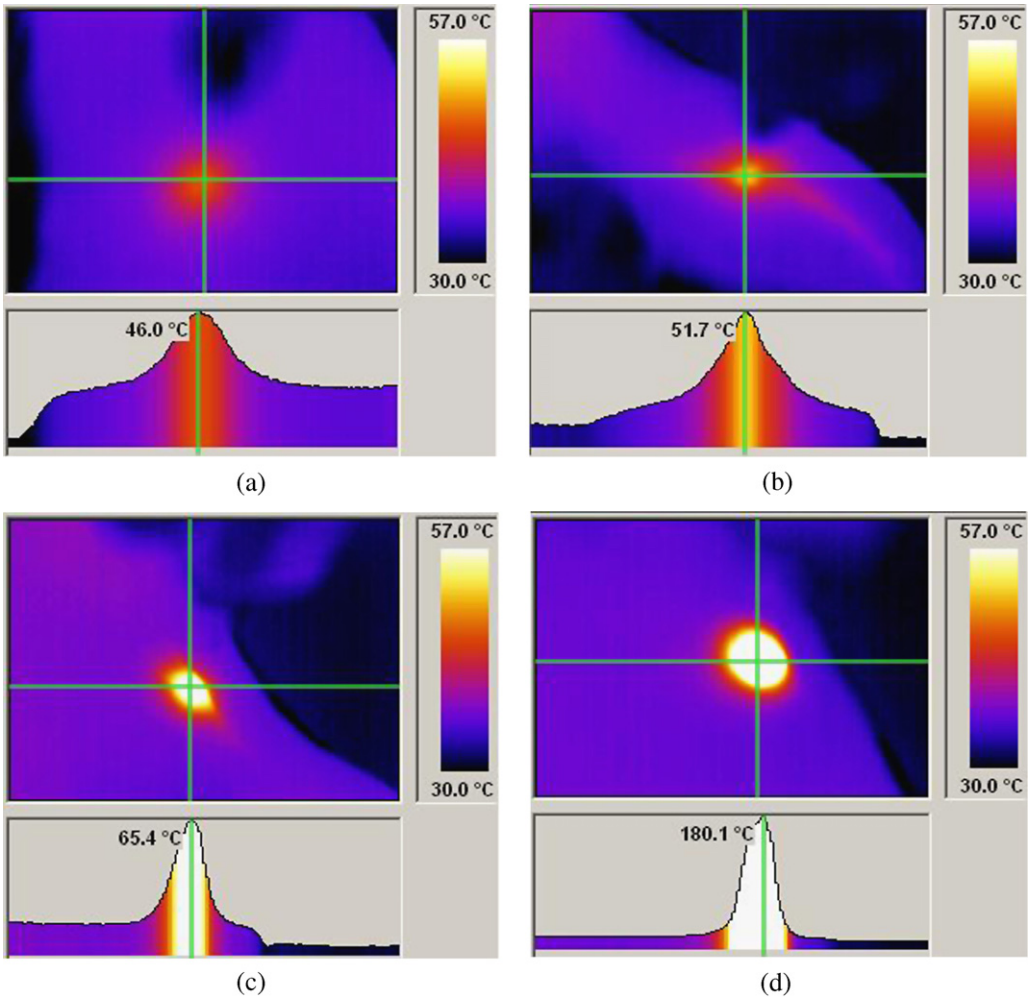

Fig. 5. Thermograms of rat's skin surface with different depth injection of nanoshells after laser irradiation during 30 s: (a) control without nanoparticles; (b) intramuscular injection of 0.1 ml of silica/gold nanoshells (depth is about 5 mm); (c) subcutaneous injection and (d) intradermal injection.

color and structure of tissue surface during irradiation time. However, the surface temperature was approximately 7° C higher than in the control measurements without nanoparticles. Computer simulation showed that the temperature in the region of nanoparticle localization could substantially exceed the surface temperature recorded by the thermal imaging system. Thus, the laser thermolysis can be achieved in the region of nanoparticle localization without damage of the surface tissues. This conclusion is confirmed by histological examinations.

The local temperature can reach or slightly exceed 60 °C with the hypodermic injection of nanoparticles. The denaturation of proteins should occur rapidly at this temperature. It can be complete or partial, reversible or irreversible. Clearly, the degree and speed of such protein denaturation depends strongly on the value and duration of temperature excess, as well as on the protein nature. The critical denaturation temperature for majority of tissue components is about 57 °C. After 15–20 s we observed the surface albication of skin followed by the thermal burn of skin.

With the intracutaneous introduction of nanoparticles, the visual changes in the biological tissue were observed for irradiation times less than 10 s. The noticeable dehydration of biological tissues begins at a temperature near 70 °C. After the water withdrawal, the dried tissue is heated rapidly to a temperature of 150 °C, at which the carbonization process begins. In short, hydrogen leaves the organic molecules and a fine dispersed carbon (soot) is formed, i.e., the carbonization occurs. The maximum value of the local temperature in this case can exceed 180 °C. This value exceeds substantially the temperature, which was observed in the experiments with the large volumes of the aqueous suspension of gold nanoparticles. We can explain this contradiction by rapid expulsion of water from the local

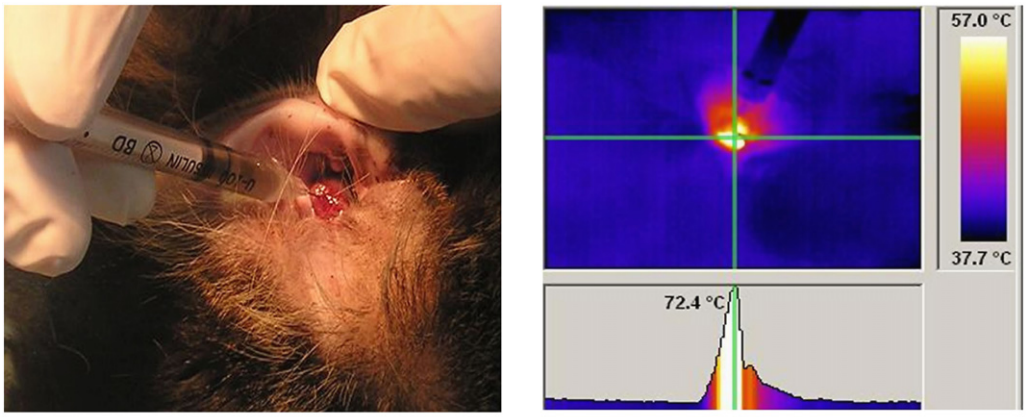

(a) (b)

Fig. 6. Photograph and thermogram of cutaneous squamous cell carcinoma of external ear canal.

section of biological tissue. The process of evaporation was observed also in the test tube. Note that the evaporation takes rather long time periods because of the large volume of liquid, and only small part of the liquid volume was actually evaporated after irradiation during 2–3 min. However, in these experiments and in a number of rare cases, we observed the formation of nanoparticle aggregates.

Laser photothermolysis of the animal spontaneous tumor

In this section, we report on some preliminary results of laser thermolysis of spontaneous tumor of skin and oral mucosa of cats and dogs. For noninvasive local temperature control in tumor region, we used the IR thermography.

During the laser hyperthermy of the spontaneous animal tumors, the infrared thermography was used for the pre-operation estimation of the tumor size, for the control of local heating and temperature under the laser radiation. Besides, the same method was used to control the processes of healing in the post-operative period and for early detection of pyoinflammatory processes. The informative content of the IR thermography was examined with diagnostics of the skin melanoma, the cancer of language, larynx, the melanoma of the pinna, the planocellular cancer, and basal cell tumor of the pinna [17]. Here we discuss the following experimental examples: two cases of the melanoma of mucosa of dogs mouth, two cases of oral squamous cell carcinoma, the cutaneous squamous cell carcinoma, and the external ear canal (Fig. 6).

Nanoparticles were injected directly into the region of tumor. In the first two cases, the treatment was stated in the late stage of pathologic process and the recovery could not be achieved. Nevertheless, we observed a period (several months) of stabilization of the cancer process and even a amelioration of clinical state during the complex application of the laser hyperthermolysis and immunotherapy [18]. In the remaining cases, after laser hyperthermy, the inflammatory burn reaction of average degree was observed, and the epithelization with the formation of scar occurred at 7–12 days. Additionally, some remission process was observed within 3–6 months; it was accomplished by the absence of metastasis during 3 months.

Conclusions

We have presented the results of computer simulation of the spatial distribution of the absorbed laser intensity, accompanied by calculation of temperature for samples, which include the absorbing nanoshells. The temperature distribution in colloidal gold solutions and on the animal skin surface was measured experimentally for two modalities: with and without injected of gold nanoparticles. It is believed that the proposed approach allows to determine the temperature in the depth of biological tissue by using thermograms of its surface.

Experiments with the laser heating of gold nanoshells allow for determination of such important parameters as the level of IR laser power density and the corresponding temperature increment caused by nanoparticles in solutions irradiated by CW or pulsed laser light. Experiments showed effective destruction of cancer cells of ear, mouth and skin by local injection of plasmon-resonant gold nanoshells followed by semiconductor laser (810 nm) irradiation. For destruction of such tumor cells, the pulse duration was about 1 μs (on–off time ratio was about 10), the average power densities were about 1–3 W/cm^2, and the laser fluencies were about 100–200 J/cm^2.

The results of laser hyperthermy at the wavelength 808 nm with using resonance nanoparticles for treatment of malignant tumors of skin and mucosa of small animals have been considered. We describe applications of silica/gold nanoshells to photothermal therapy of cancer exemplified by spontaneous tumor of cats and dogs. Effect of nanoparticles on the laser photothermolysis of tumor of dogs and cats was studied *in vivo* by the local injection of nanoparticles around the tumor. In general, the total experiment included the following cases: the cutaneous squamous cell carcinoma of external ear canal, the squamous cell carcinoma of oral mucous, the basal cell cutaneous tumor of external ear canal, the malignant melanoma of oral mucosa. Some positive therapeutic effect was observed as a result of undertaken complex therapy.

Acknowledgments

This research was partially supported by grants from RFBR (Nos. 07-02-01434a and 05-02-16776a), the Ministry of Science and Education of the Russian Federation (Nos. 1.4.06, RNP.2.1.1.4473, Contracts Nos. 02.512.11.2034 and 02.513.11.3043), and CRDF BRHE RUXO-006-SR-06. BK was supported by grants from the President of the Russian Federation (No. MK 2637.2007.2), RFBR (Nos. 07-04-00301a and 07-04-00302a), and INTAS YS Fellowship (No. 06-1000014-6421).

Zusammenfassung

NIR-photothermische Lasertherapie von Tumoren unter Verwendung von Gold-Nanoteilchen: Computersimulationen und Experimente

Wir beschreiben Applikationen von Silica (Kern)/Gold(Hülle)-Nanopartikel für die photothermische Therapie spontaner Tumore bei Katzen und Hunden. Die Laser-Bestrahlungsparameter wurden durch vorausgehende Experiments an Ratten optimiert. Die Temperaturverteilung im Gewebe und in wässrigen Proben wurden mit einer Thermokamera gemessen. Es wird gezeigt, dass die Temperaturverteilung, mit der Thermokamera aufgenommen, im Volumen der Nanopartikelanreicherung die gemessene Oberflächentemperatur substantiell übersteigt. Wir demonstrieren die effektive Zerstörung von Tumorzellen durch lokale Injektion von Plasmon-resonante Gold-Nanopartikel (nanoshells) und Bestrahlung mit einem Diodenlaser bei 808 nm.

Schlüsselwörter: Gold-Nanopartikel; Silica/Gold „nanoshells"; Plamon-Resonanz; Tumor; Photothermische Lasertherapie

Resùmen

Terapia fototérmica láser en el IR cercano con nanopartículas de oro aplicada al cáncer: Simulaciones computacionales y experimental

En este trabajo se describe el uso de nanoparticulas de silica (núcleo)/oro (cubierta) para la terapia fototérmica de tumores espontáneos en perros y gatos. Los parámetros de irradiación láser fueron optimizados en experimentos preliminares utilizando ratas de laboratorio. La distribución de la temperatura en muestras de tejido y muestras solubles fue medida mediante un sistema térmico de proyección de imágenes. De esta manera, se demostró que la temperatura en la región de localización de los nanoparticulas excede substancialmente la temperatura superficial registrada a través del sistema térmico de proyección de imágenes. Más aún, se observó que la inyección local de plasmón resonante mediante nanoparticulas de oro seguida de una radiación con un láser de diodo de 808 nm produce una destrucción efectiva de las células tumorales.

Palabras clave: Nanopartículas de oro; Silica/oro "nanoshells"; Resonancia de plasmón; Cáncer; Terapia Fototérmica Láser

References

[1] Yonzon CR, Zhang X, Zhao J, van Duyne RP. Surface-enhanced nanosensors. Spectroscopy 2007;22:42–56.
[2] Kubik T, Bogunia-Kubik K, Sugisaka M. Nanotechnology on duty in medical applications. Curr Pharm Biotechnol 2005;22:17–33.
[3] Gobin AM, Lee MH, Halas NJ, James WD, Drezek RA, West JL. Near infrared resonant nanoshells for combined optical imaging and photothermal cancer therapy. Nano Lett 2007.
[4] Huang X, Jain PK, El-Sayed MA. Plasmonic photothermal therapy (PPTT) using gold nanoparticles. Lasers Med Sci 2007.
[5] Khlebtsov BN, Zharov VP, Melnikov AG, Tuchin VV, Khlebtsov NG. Optical amplification of photothermal therapy with gold nanoparticles and nanoclusters. Nanotechnology 2006;17:5167–79.
[6] Harris N, Ford MJ, Cortie MB. Optimization of plasmonic heating by gold nanospheres and nanoshells. J Phys Chem B 2006;110:10701–7.
[7] O'Neal DP, et al. Photo-thermal tumor ablation in mice using near infrared-absorbing nanoparticles. Cancer Lett 2004;2009:171–6.
[8] Glomm WR. Functionalized gold nanoparticles for application in biotechnology. J Dispers Sci Technol 2005;26:389–414.
[9] Bogatyrev VA, Dykman LA. Gold nanoparticles: preparation, functionalization, and applications in

biochemistry and immunochemistry. Russ Chem Rev 2007;76:181–94.
[10] Khlebtsov NG, Melnikov AG, Bogatyrev VA, Dykman LA. Optical properties and biomedical applications of nanostructures based on gold and silver bioconjugates. In: Videen G, Yatskiv YS, Mishchenko MI, editors. Photopolarimetry in remote sensing. Nato science series, ii: mathematics, physics, and chemistry, vol. 161. Dordrecht: Kluwer; 2004. p. 265–308.
[11] Hirsch LR, Gobin AM, Lowery AR, Tam F, Drezek RA, Halas NJ, et al. Metal nanoshells. Ann Biomed Eng 2006;34:15–22.
[12] Kalele S, Gosavi SW, Urban J, Kulkarni SK. Nanoshell particles: synthesis, properties and applications. Curr Nanosci 2006;91:1038–52.
[13] Paciotti GF, Myer L, Weinreich D, Goia D, Pavel N, McLaughlin RE, et al. Colloidal gold: a novel nanoparticle vector for tumor directed drug delivery. Drug Deliv 2004;11:169–83.
[14] Irani GB, Huen T, Wooten F. Optical constants of silver and gold in the visible and vacuum ultraviolet. J Opt Soc Am 1971;61:128–9.
[15] Otter M. Optische konstanten massiver metalle. Z Phys 1961;161(1–2):163–78.
[16] Johnson PB, Christy RW. Optical constants of noble metals. Phys Rev B 1973;12:4370–9.
[17] Rosenfeld LG, Kolotilov NN. Remote infrared thermography in oncology. Onkologiya 2001;3:103–6 [in Russian].
[18] Terentyuk GS, Maksimova IL, Tuchin VV, Zharov VP, Khlebtsov BN, Bogatyrev VA, et al. Application of gold nanoparticles to X-ray diagnostics and photothermal therapy of cancer. In: Zimnyakov DA, Khlebtsov NG, editors. Coherent optics of ordered and random media VII. Proceedings of the SPIE 2007, vol. 6536, p. 1–12 (65360B).